ELSEVIER

Ceramics International 28 (2002) 487–493

CERAMICS INTERNATIONAL

www.elsevier.com/locate/ceramint

Influence of *in situ* phase formation on microstructural evolution and properties of castable refractories

H. Sarpoolaky[1], K.G. Ahari, W.E. Lee*

Department of Engineering Materials, University of Sheffield, Mappin Street, Sheffield S1 3JD, UK

Received 3 September 2001; received in revised form 20 September 2001; accepted 3 October 2001

Abstract

The microstructural evolution on firing and quenching two commercial composition castable refractories, a vibratable ultralow cement castable and an *in situ* spinel low cement castable, was fully characterized and related to high-temperature properties. The emergence of refractory phases such as calcium hexaluminate, magnesium aluminate spinel and mullite was observed to have beneficial effects on hot bend strength and refractoriness under load due to the development of morphologies which interlocked other phases and to pore filling from expansile reactions.

Keywords: D. Mullite; D. Spinel; Refractory castables; In situ; Calcium hexaluminate

1. Introduction

Low cement castables (LCC's) and ultra-low cement castables (ULCC's) are used extensively in refractories applications due to their excellent properties and ease of installation [1]. Most castables are based on calcium aluminate cement (CAC) bonding although there is a trend away from lime-containing systems due to its fluxing action at high temperatures in aluminosilicates [2]. The general form of the microstructural evolution on firing CAC-bonded castables is well understood [3]. Hydration starts immediately on mixing the castable with water forming different calcium aluminate hydrates with various morphologies depending on the water/cement ratio, curing condition (especially temperature and relative humidity) and impurities. All hydrated compounds dehydrate by 550 °C [4] forming anhydrous, extremely fine active lime and alumina which react to produce calcium aluminates. The fine fractions of the matrix phases, including products of hydration, initially react among themselves and at higher temperature they, or their reaction products, may react with the coarser aggregate phases. In conventional CAC-bonded castables $C_{12}A_7$, CA and CA_2 form in this sequence with increasing temperature until >1300 °C when CA_2 reacts with alumina to form hexagonal platelets of CA_6 [5]. These reactions occur during the first in-service heating after installation. By proper control of the castable formulation formation of beneficial phases, such as calcium hexaluminate (CA_6), spinel and mullite can occur in the refractory matrix *in situ* [6]. The reactions leading to these in situ phases have associated volume changes which may tighten the microstructures texture [7]. Furthermore, the resulting phases often have acicular or elongated morphologies which may interlock and link other phases leading to improved properties [8,9].

In *in situ* spinel forming castables fine MgO and Al_2O_3 react to form spinel which (depending on the other matrix phases present) has a variety of morphologies and which is known to improve slag resistance [10,11]. Microsilica is generally used to improve the flow behaviour of these castables leading to liquid formation via low melting CAS phases at elevated temperatures [12,13]. Lime/silica (C/S) ratio is an important factor in determining the amount and viscosity of the liquid as well as hot strength and creep resistance of the refractory [14]. ULCC's have increased refractoriness and improved high temperature properties due to their lower CAC and thus lime contents [15–17]. Several low melt-

* Corresponding author. Tel.: +44-114-2225474; fax: +44-114-2225943.

E-mail address: w.e.lee@sheffield.ac.uk (W.E. Lee).

[1] Permanent address: Department of Engineering Materials, Iran University of Science and Engineering, Narmak, Tehran, Iran.

0272-8842/02/$22.00
PII: S0272-8842(01)00121-3

ing eutectics are present in the $CaO–Al_2O_3–SiO_2$ (CAS) ternary system while compositions in the high-alumina part of the Al_2O_3–MgO–CaO (AMC) ternary show high refractoriness due to the high temperatures of the invariant points in this region of the diagram. Nonetheless, SiO_2 has deleterious effects on both CAS and AMC systems and degrades their high temperature properties [18]. As microsilica is inevitably needed for casting, efforts were made to decrease CaO content limiting formation of low melting CAS phases. Cement was substituted with superfine alumina to develop a network of *in situ* mullite needles in the castable bond due to reaction of alumina and silica around 1400 °C. The elongated needle-like mullite crystals grow and lock the structure to create a strong refractory bond system so improving the mechanical properties of the castable [19,20].

The purpose of present work is to study the influence of *in situ* mullite and spinel formation on microstructural evolution and high-temperature properties of two commercial castables.

2. Experimental procedure

Two commercial castables were examined. The first was a vibratable ultralow cement alumina castable (Al-ULCC) made of sintered and fused alumina aggregates and hydratable alumina (HA), fumed silica (~5 wt.%) and calcium aluminate cement (~1%). The second was a self-flowing, *in situ* spinel, low cement castable (Sp-LCC) based on bauxite, fused and tabular alumina as aggregates and hydratable alumina, magnesia (~10%), fumed silica and calcium aluminate cement (~4 wt.%). Table 1 shows the chemical compositions of the castables supplied by the manufacturer. The samples were cast in moulds after mixing with controlled water addition (Table 1), wrapped in plastic and cured at room temperature for 24 h. They were then removed from the moulds and cured for a further 24 h at room temperature and dried at 110 °C for another 24 h. They were fired at 1000, 1200, 1400, 1500 and 1600 °C with 3 h dwell and then furnace cooled. For X-ray diffraction (XRD) the samples were crushed and sieved <100 μm and the spectra recorded on a unit (model No. PW1050, Philips Electronic Instruments, Mahwah, NJ, USA) operating at 30 mA and 40 kV, using Ni-filtered CuK_α radiation. A scanning electron microscope (series 2 SEM, Camscan Electron Optics, UK) equipped with an energy-dispersive spectroscopy (EDS) analyser (model AN10000, Link Systems, High Wycombe, Bucks, UK) was used for secondary electron imaging (SEI) and back-scattered electron imaging (BSI). Mercury porosimetry was used to measure open pore size distributions (model 9320 pore sizer, Micromeritics Instrument Corp., Norcross, GA, USA). Refractoriness under load (RUL) testing was carried out by Corus (Teesside Technology Centre, UK) according to DIN standard EN 993-8 on 50×50 mm cylinders under 0.2 MPa in air. Samples were prefired 3 h at 1000 °C and cooled to room temperature prior to testing. During the test samples were heated to temperature at 3 °C/min. Hot modulus rupture (HMOR) was measured by Vesuvius Premier, Worksop, UK in 3-point bending on 25×25×152 mm samples according to ASTM C 583 from 1000 to 1600 °C with 3 h dwell at the test temperature.

Table 1
Chemical analysis (wt.%) of the commercial castables

Castable type	Al-ULCC	Sp-LCC
SiO_2	4.9	2
CaO	0.3	1
MgO	Trace	9.7
Fe_2O_3	Trace	0.4
TiO_2	–	0.6
Alkalis	0.3	0.3
Al_2O_3	94.2	86.0
Water requirement	3.5 l/100 kg	6 l/100 kg

3. Results and discussion

3.1. X-ray diffraction

XRD indicated α-alumina was the major crystalline phase in the dried Al-ULCC together with minor β-alumina. The β-alumina had disappeared after firing at 1400 °C and alumina was the only crystalline phase present after firing at 1600 °C. In the *in situ* spinel castable (Sp-LCC) α-alumina and MgO were the main phases in the dried samples and those fired at 1000 °C. Spinel was found after firing at 1200 °C and increasingly formed at the expense of MgO upon heating to 1600 °C as only spinel and alumina were detected at this temperature.

3.2. Microstructural evolution

3.2.1. After drying at 110 °C

The general microstructures of both castables after drying at 110 °C were similar except that no MgO was present in the Al-ULCC. Fumed silica was well dispersed in both samples while hydratable alumina (HA) and CAC cement (C) were partially agglomerated. Fig. 1 shows the microstructure of Sp-LCC after drying at 110 °C revealing bauxite (B), tabular and fused alumina aggregates (TA, FA) with magnesia (M), fine alumina (A) and agglomerates of CAC and HA in the matrix.

3.2.2. Microstructural evolution on firing

3.2.2.1. Al-ULCC. After firing at 1000 °C the Al-ULCC microstructure reveals TA aggregates with dehydrated

agglomerates of HA and CAC much like in Fig. 1. Fumed silica is well dispersed within the matrix with no evidence of CAS formation. The cement agglomerates typically contain CA and CA_2 at this temperature. Increasing the firing temperature to 1200 °C significantly changed the microstructure (Fig. 2). Low melting calcium aluminium silicate (CAS) liquid formed in the matrix leaving bright CAS-rich regions around the cement agglomerates, while dispersed microsilica in the bond started to react with alumina from HA agglomerates forming an aluminosilicate (AS) rim around them. CA_2 forms in the cement agglomerates due to reaction of CA with alumina.

Heating at 1400 °C revealed evidence of extensive CAS liquid formation in the bond (Fig. 3). The liquid viscosity decreases on increasing temperature facilitating liquid phase sintering and helping to bond the aggregates together. The CAS liquid has also penetrated the outer TA aggregate pores causing a bright ring around them (Fig. 3a). After firing at 1500 °C (Fig. 4) Al-ULCC shows well-developed mullite crystals formed inside the HA agglomerates suggesting that the microsilica reacted with the alumina from HA agglomerates forming aluminosilicates (bright rim in Fig. 2) which formed mullite at 1400 °C. Consistent with the CAS ternary phase diagram no CA_6 was detected [21]. After firing at 1400 °C and above the bond phase is predominantly alumina with some mullite crystals held together by the solid amorphous products of cooling the CAS melt. Firing at 1600 °C did not change the phases present but a reduced mullite content suggests it is beginning to redissolve in the CAS liquid.

3.2.2.2. Sp-LCC. After firing at 1000 °C the microstructure is similar to that observed after drying at 110 °C (Fig. 1) containing cement (C) and hydratable alumina (HA) agglomerates and the FA and TA aggregates as well as sintered MgO (M). Some MgO crystals

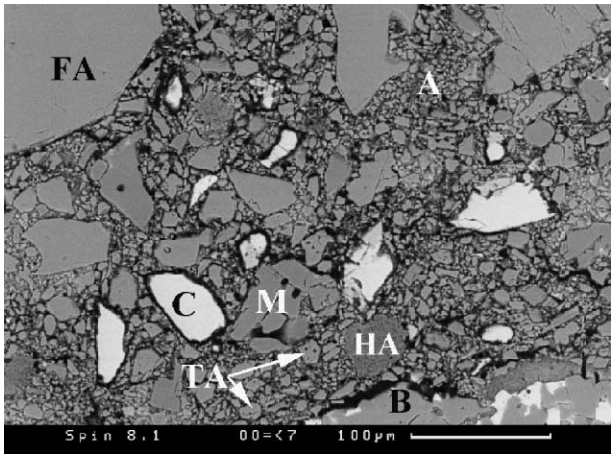

Fig. 1. BEI of the Sp-LCC after drying at 110 °C showing B, TA, FA aggregates and the matrix containing magnesia (M), fine alumina (A) and agglomerates of CAC cement (C) and hydratable alumina (HA).

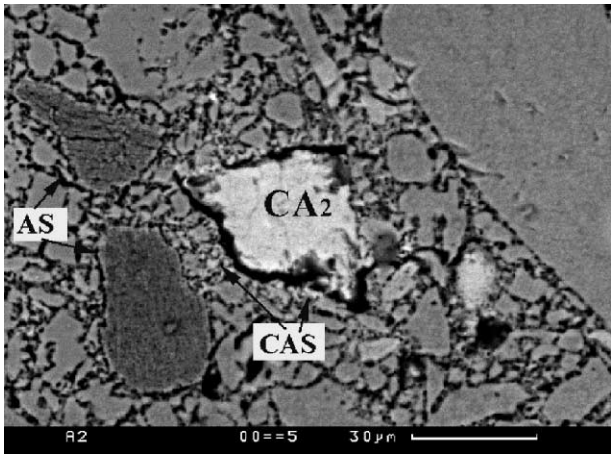

Fig. 2. BEI of the Al-ULCC fired 3 h at 1200 °C showing HA agglomerate with light aluminosilicate rim (AS) and bright CAS phases around the cement (CA_2) and in the matrix.

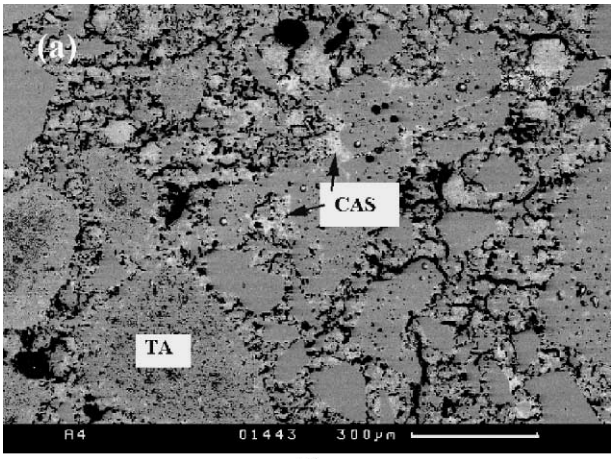

(a)

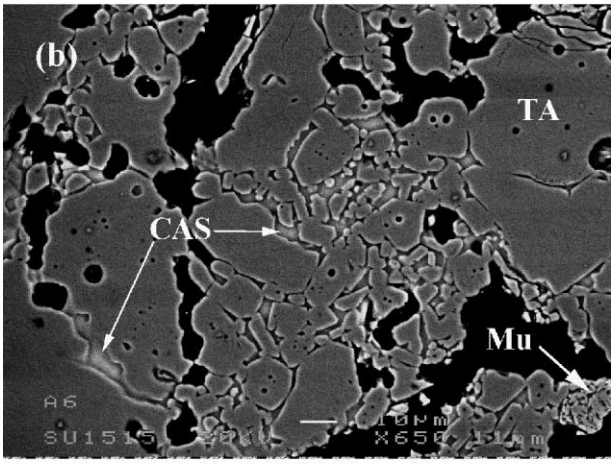

(b)

Fig. 3. BEI of the Al-ULCC fired at 1400 °C showing TA, FA grains held together by CAS melt (a) low and (b) high magnification revealing large connected pores and fine mullite (Mu).

were surprisingly large at 30–100 μm with lime as well as Cr, Ti and Fe oxides as grain boundary impurities revealing it is a sintered product. After firing at 1200 °C (like Al-ULCC) the microstructure changed considerably as low melting CMAS phases led to liquid generation and spinel began to form on fine alumina particles in the matrix by reaction of the fine fractions (Fig. 5).

After firing at 1400 °C the bond converted entirely to spinel with no alumina left in the matrix although some MgO remains (Fig. 6). A few MgO grains located in silica-rich areas had forsterite (Mg_2SiO_4) rims. Spinel formed with various morphologies including angular/facetted crystals (centre of Fig. 6) and tuber-like (left side of Fig. 6). The bright CMAS phases in Fig. 6 are probably liquid at 1400 °C. After firing at 1500 °C most MgO grains have been consumed except those covered by forsterite suggesting it protected them and delayed spinel formation. Spinel formation was completed after firing at 1600 °C with no free magnesia detected (Fig. 7). The microstructure consisted of alumina grains surrounded by a spinel-rich matrix including some CA_6 and CMAS containing small amounts of TiO_2 and other impurities arising from the bauxite aggregates and MgO. These are likely to decrease the CMAS liquid viscosity [22].

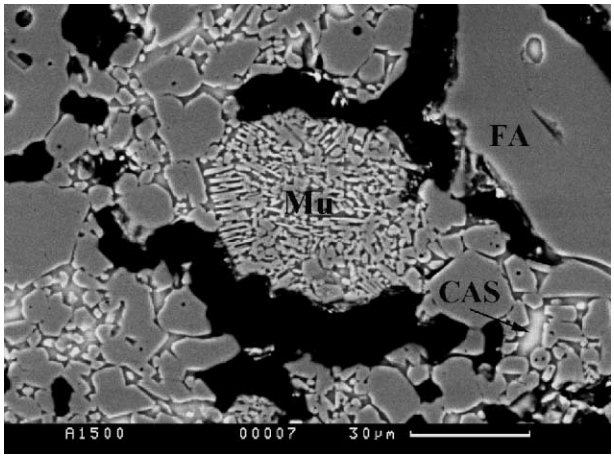

Fig. 4. BEI of the Al-ULCC fired at 1500 °C showing TA, FA grains, black pores, elongated mullite crystals (Mu) in HA relicts and CAS in the bond.

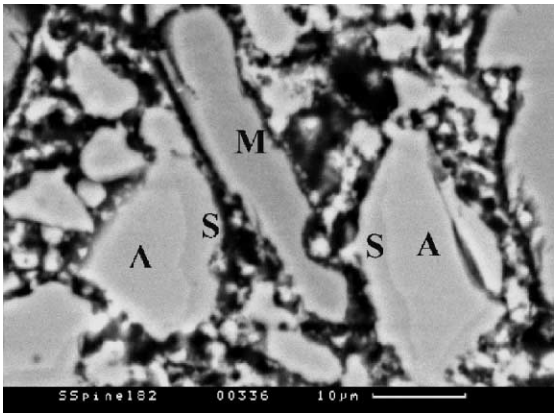

Fig. 5. BEI of the Sp-LCC fired at 1200 °C showing darker spinel rim (S) formed on the edges of alumina particles (A) but not MgO (M).

3.2.3. Pore size distribution

Fig. 8 shows pore size distributions from the castables after firing at 1000, 1400 and 1600 °C and Table 2 median pore size, bulk density and porosity data. The smaller initial pore size and porosity level of Al-ULCC compared to Sp-LCC after firing at 1000 °C is related to the lower volume of water used in fabrication (Table 1) which leaves open pores behind on its escape. However, pores in Al-ULCC increased in size more than those in Sp-LCC after firing at 1200–1600 °C while the porosity level decreased more. This is believed to be due to better sintering behaviour in Sp-LCC due to higher levels of liquid formation (e.g. compare Figs. 3 and 6) associated

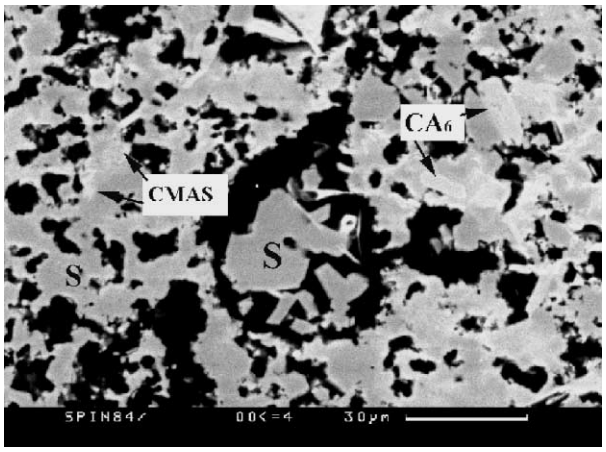

Fig. 6. Microstructure of Sp-LCC fired at 1400 °C showing spinel bond (S) with various morphologies, CA_6 and CMAS phases.

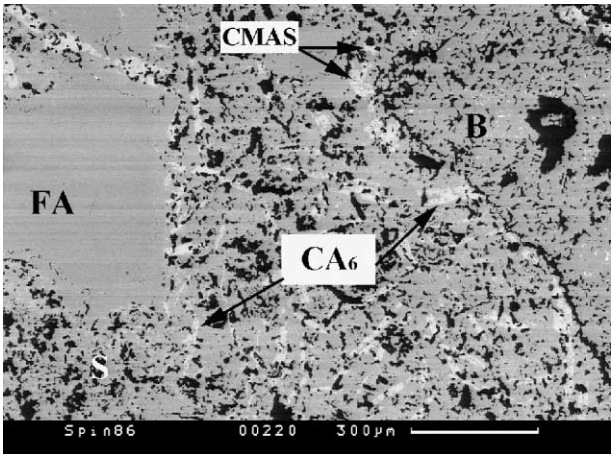

Fig. 7. BSI of Sp-LCC fired at 1600 °C showing the alumina grains held together by a spinel-rich matrix, including TiO_2-containing CA_6 and CMAS.

Table 2
Porosity/density data after firing at 1000–1400 °C

Castable	Median pore size (μm), BD (g/cm^3) and P (vol.%) after firing at:								
	1000 °C			1400 °C			1600 °C		
Al-ULCC	0.34	3.24	11.16	3.7	3.5	6.7	12.9	3.58	7.07
Sp-LCC	0.65	3.06	19.71	1.7	2.84	21.44	3.1	3.5	13.52

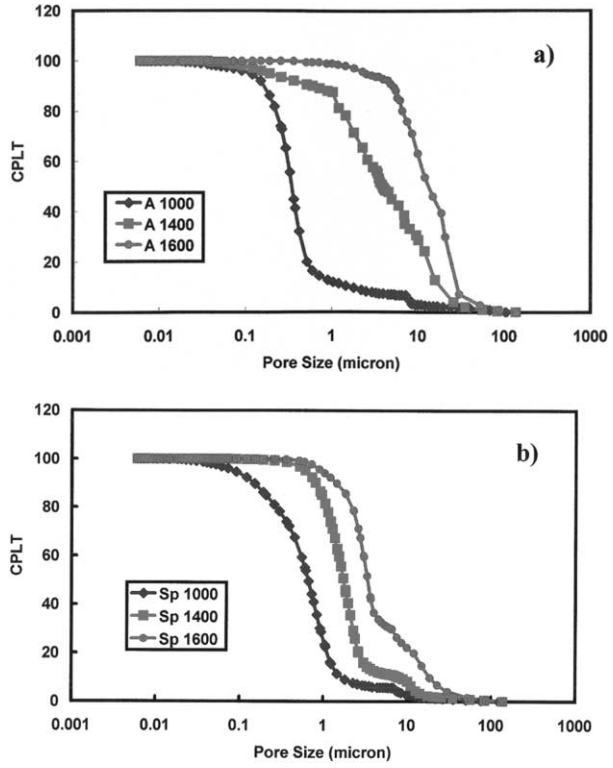

Fig. 8. Pore size distributions of (a) Al-ULCC and (b) Sp-LCC after firing at 1000, 1400 and 1600 °C.

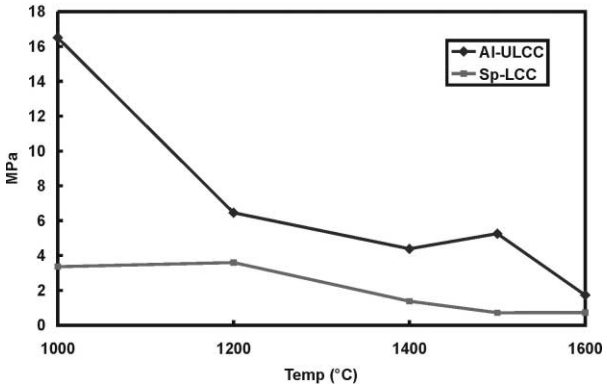

Fig. 9. HMOR of castables fired between 1000 and 1600 °C.

with impurities from the magnesia and bauxite (alkalis, TiO_2, Fe_2O_3 and silica). CAS liquid filled many pores as well as facilitating coalescence of others (Figs. 3b and 4). Porosity levels remain high (over 20%) in Sp-LCC to 1400 °C (see Fig. 6) but decrease substantially by 1600 °C. This is likely explained by volume expansions associated with formation of spinel and CA_6 (Fig. 7) in the matrix as well as liquid generation.

3.3. Property measurements

3.3.1. HMOR

Al-ULCC has a much higher HMOR than Sp-LCC after firing to 1000 °C (Fig. 9) attributable to its lower porosity level (Table 1) and CAC content leading to less low melting CAS phases [16,19]. However, it showed a sharp decrease in HMOR on heating to 1200 °C attributable to more extensive formation of CAS liquid at this temperature consistent with the microstructures (Fig. 2) and density data (Table 2). This decrease continued to 1400 °C but at a lower rate and HMOR then increased in samples fired to 1500 °C. This is surprising since the higher temperature might be expected to increase the volume of liquid and lower its viscosity. However, the formation of platey mullite in the matrix at these temperatures (Fig. 4) could explain the retention of HMOR while the decrease after firing to 1600 °C is due partly to the re-dissolution of mullite in the CAS melt. Sp-LCC showed a slight increase in HMOR from 1000 to 1200 °C followed by a decrease to 1500 although this level was maintained at 1600 °C. The spinel which starts to form between 1000 and 1200 °C (Fig. 5) is known to improve the hot strength of such castables [5]. The HMOR decrease between 1200 and 1500 °C is due to CMAS melt formation and decreased viscosity while CA_6 formation (Fig. 7) may explain the retention of hot strength from 1500 to 1600 °C. The HMOR values of the both castables are similar at 1600 °C in spite of the greater amount of melt believed to be present in Sp-LCC.

3.3.2. RUL

RUL data for the two castables (Fig. 10) were similar, revealing a small expansion up to 1100 °C while Sp-LCC showed better behaviour than Al-ULCC from 1100 to 1500 °C. However, Sp-LCC showed a particularly poor RUL response between 1500 and 1600 °C. In refractory castables deformation of the matrix system is believed to play the major role in their high temperature properties [16]. Generally, HMOR and RUL behaviour of refractories can be attributed to deformation of the matrix since the aggregates are mostly rigid at the test temperature [23]. The matrix of Sp-LCC contains fine

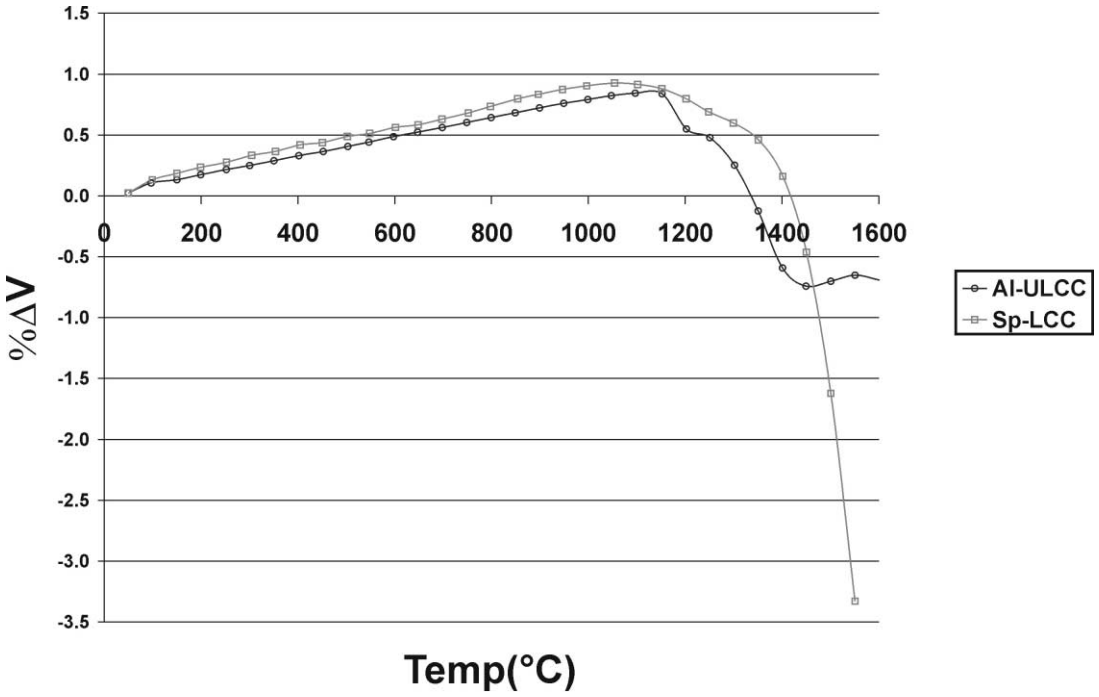

Fig. 10. Refractoriness under load (RUL) data for both castables.

alumina, magnesia, CAC and silica which react with impurities from bauxite and MgO to give a fluid CMAS liquid leading to the poor RuL observed at high temperature. The matrix of Al-ULCC contains fine alumina which reacted with CaO and SiO_2 to form CAS at 1200 °C affecting its pore size distribution and HMOR. Mullite formation is associated with a volume increase [7] which leads to pore filling and the acicular, interlocking morphology leads to improved RUL and HMOR at 1400 °C and above. Recently, Zawarah and Khalil [24] studied the effect of mullite formation on properties of refractory castables containing different amount of alumina/silica and CAC contents. Consistent with the present work they showed that mullite formed at 1500 °C in the matrix of castables containing 2% CAC leading to outstanding thermo-mechanical properties.

4. Conclusions

- High-temperature properties of Al-ULCC were generally better than those of Sp-LCC.
- CAS formation at 1200 °C resulted in increased pore size and a dramatic decrease in HMOR for Al-ULCC.
- *In situ* mullite formation above 1400 °C led to improved HMOR in Al-ULCC.
- Formation of *in situ* spinel and CA_6 in Sp-LCC compensated the deleterious effect of its higher CAC content on HMOR and RUL and gave it better RUL than Al-ULCC from 1200 to 1400 °C.
- The poor RUL of Sp-LCC above 1400 °C was likely due to the presence of impurities from the bauxite and MgO increasing fluidity of the CMAS melt.

References

[1] J. Yamada, S. Sakaki, K. Kasai, H. Ishimatsu. Application technology of monolithic refractories in NSC, in: Proceedings of the Unified Int. Tech. Conf. on 'Refractories' (UNITECR '95), Kyoto, Japan, 1995, pp. 277–84.
[2] K.G. Ahari, J.H. Sharp, W.E. Lee, Hydration of refractory oxides in castable bond systems: I, alumina, magnesia, and alumina-magnesia mixtures, J. Eur. Ceram. Soc. 22(4) (2002) 495–503.
[3] W.E. Lee, W. Viera, S. Zhang, K.G. Ahari, H. Sarpoolaky, C. Parr, Castable refractory concretes, Int. Mater. Rev., in press.
[4] A. Nishikawa, Technology of Monolithic Refractories, Plibrico Japan Company Limited, 1984.
[5] F. Simonin, C. Olagnon, S. Maximilien, G. Fantozzi, Thermomechanical behaviour of high-alumina refractory castables with synthetic spinel additions, J. Am. Ceram. Soc. 83 (10) (2000) 2481–2490.
[6] W.E. Lee, R.E. Moore, Evolution of in situ refractories in the 20th century, J. Am. Ceram. Soc. 81 (6) (1998) 1385–1410.
[7] F.N. Cunha, R.C. Bradt, Reactions of constituents for in situ bonds of $MgAl_2O_4$, Mg_2SiO_4 and $3Al_2O_3.2SiO_2$ in refractories, in: ISS-57th Electric Furnace Conference, Pittsburgh, Pa, USA, 1999, pp. 143–152.
[8] M. Fuhrer, A. Hey, W.E. Lee, Microstructural evolution in self-forming spinel/calcium aluminate-bonded castable refractories, J. Eur. Ceram. Soc. 18 (7) (1998) 813–820.
[9] Y. Urita, M. Sugawara, M. Kataoka, K. Yamaguchi, Development of self-forming spinel castable for steel ladle, 39th Int. Coll. on Refr. in Stahl&Eisen (special vol.) 10 (1996) 108–111.
[10] S. Asou, Y. Mikami, S. Harada, Refractory maintenance

technology for steel teeming ladles, Taikabutsu Overseas 16 (4) (1996) 49–54.
[11] P. Korgul, D.R. Wilson, W.E. Lee, Microstructural analysis of corroded alumina-spinel-castable refractories, J. Eur. Ceram. Soc. 17 (1997) 77–84.
[12] B. Myhre, Microsilica a versatile refractory raw material (Elkem Report), Presented at The Indian Refractories Congress, 1994.
[13] S. Zhang, W.E. Lee, Use of phase diagrams in studies of refractories corrosion, Int. Mater. Rev. 45 (2) (2000) 41–58.
[14] A. Rendtel, H. Hubner, Interpretation of the creep behavior of low cement refractory castables based on the properties of the interaggregate glassy phase, in: Proceedings of the Unified Int. Tech. Conf. on 'Refractories' (UNITECR '97), New Orleans, USA, 1997, pp. 71–80.
[15] B. Myhre, Hot strength and bond-phase relations in low and ultralow-cements for high technology castables, in: Proceedings of the Unified Int. Tech. Conf. on 'Refractories' (UNITECR '93), Sao Paulo, Brazil, 1993, pp. 583–594.
[16] H.H. Strothmann, H. Hubner, A. Rendtel, V.C. Pandolfelli, J.A. Rodrigues, High-temperature performance of cement-free and low cement alumina castables, in: Proceedings of the Unified Int. Tech. Conf. on 'Refractories' (UNITECR '95), Kyoto, Japan, 1995, pp. 343–350.
[17] B. Myhre, K. Sunde, Alumina based castables with very low content of hydraulic compounds. Part II: strength and high-temperature reaction of no-cement castables with hydraulic cement and microsilica, in: Proceedings of the Unified Int. Tech. Conf. on 'Refractories' (UNITECR '95), Kyoto, Japan, 1995, pp. 317–324.
[18] A.A. Wereszczac, T.P. Kirkland, Creep of CaO/SiO_2-containing MgO refractories, J. Mater. Sci. 34 (1999) 215–227.
[19] M.H. Hundere, B. Myhre, Substitution of reactive alumina with microsilica in low cement and ultra low cement castables, in: Proceedings of the Unified Int. Tech. Conf. on 'Refractories' (UNITECR '97), New Orleans, USA, 1997, pp. 91–100.
[20] B. Sandburg, B. Myhre, Castables in the system $MgO–Al_2O_3–SiO_2$, in: Proceedings of the Unified Int. Tech. Conf. on 'Refractories' (UNITECR '95), Kyoto, Japan, 1995, pp. 173–79.
[21] E.M. Levin, C.R. Robbins, H.F. McMurdie, Phase Diagrams for Ceramics, Fig. 630, Am. Ceram. Soc, Columbus, OH, 1964.
[22] E.T. Turkdogan, Physicochemical Properties of Molten Slags and Glasses, The Metal Society, London, UK, 1983.
[23] W.R. Alder, J.S. Masaryk, Compressive stress/strain measurement of monolithic refractories at elevated temperatures, in: R.E. Fisher (Ed.), New Developments in Monolithic Refractories, Advances in Ceramics, Am. Ceram. Soc, Columbus, USA, 1985, pp. 97–109.
[24] M.F. Zawarah, N.M. Khalil, Effect of mullite formation on properties of refractory castables, Ceram. Int. 27 (6) (2001) 689–694.